Propionibacterium acnes and *Staphylococcus lugdunensis* Cause Pyogenic Osteomyelitis in an Intramedullary Nail Model in Rabbits

Abhay Deodas Gahukamble,[a] Andrew McDowell,[b]* Virginia Post,[a] Julian Salavarrieta Varela,[a] Edward Thomas James Rochford,[a] Robert Geoff Richards,[a] Sheila Patrick,[b] Thomas Fintan Moriarty[a]

AO Research Institute Davos, Davos, Switzerland[a]; Centre for Infection and Immunity, Queen's University, Belfast, United Kingdom[b]

Propionibacterium acnes and coagulase-negative staphylococci (CoNS) are opportunistic pathogens implicated in prosthetic joint and fracture fixation device-related infections. The purpose of this study was to determine whether *P. acnes* and the CoNS species *Staphylococcus lugdunensis*, isolated from an "aseptically failed" prosthetic hip joint and a united intramedullary nail-fixed tibial fracture, respectively, could cause osteomyelitis in an established implant-related osteomyelitis model in rabbits in the absence of wear debris from the implant material. The histological features of *P. acnes* infection in the *in vivo* rabbit model were consistent with localized pyogenic osteomyelitis, and a biofilm was present on all explanted intramedullary (IM) nails. The animals displayed no outward signs of infection, such as swelling, lameness, weight loss, or elevated white blood cell count. In contrast, infection with *S. lugdunensis* resulted in histological features consistent with both pyogenic osteomyelitis and septic arthritis, and all *S. lugdunensis*-infected animals displayed weight loss and an elevated white blood cell count despite biofilm detection in only two out of six rabbits. The differences in the histological and bacteriological profiles of the two species in this rabbit model of infection are reflective of their different clinical presentations: low-grade infection in the case of *P. acnes* and acute infection for *S. lugdunensis*. These results are especially important in light of the growing recognition of chronic *P. acnes* biofilm infections in prosthetic joint failure and nonunion of fracture fixations, which may be currently reported as "aseptic" failure.

Implant-related osteomyelitis is a serious complication of joint replacement and fracture fixation procedures. In the majority of cases, these infections are caused by bacterial species that are either permanent or transient members of the human microbiota. Of the different bacterial species present on the human skin, only a small number are frequently associated with implant-related osteomyelitis. One of the most common causative microorganisms is *Staphylococcus aureus*, which causes an acute infection characterized by fever, localized swelling, and osteolysis (1, 2). In contrast, the exact role played by other less virulent members of the skin microbiota in medical device-related infections, including the Gram-positive anaerobic-to-aerotolerant bacterium *Propionibacterium acnes* and coagulase-negative staphylococci (CoNS), has historically been less clear; these organisms were previously dismissed as contaminants when cultured from clinical specimens (3–5).

"Aseptic" implant failure is thought to result from periprosthetic osteolysis driven by wear debris arising from the implant materials (6). There is, however, a growing recognition that bacteria are an underestimated cause of subacute and chronic bone infections, aseptic loosening of implants, and arthrodesis after osteosynthesis (7–11). In particular, *P. acnes* is being increasingly recognized as a primary pathogen in relation to prosthetic shoulder implant infection (12), but it has also been linked to other medical device-related infections, including those associated with prosthetic hip joints and heart valves, as well as central nervous system shunts (13–15). In keeping with this pathogenic capacity, whole-genome sequencing has revealed the presence of multiple putative virulence determinants, including phase- and antigenically variable adhesins, as well as multiple cohemolysin CAMP factors (16). In contrast, *Staphylococcus lugdunensis* appears to be an unusually virulent CoNS species (17, 18) that has been linked to a wide range of acute infections, including those associated

with prosthetic joints (19, 20), osteomyelitis (21, 22), septic arthritis (23), soft tissue infections (24), and infective endocarditis (25). Despite this, we still have a relatively limited understanding of the role and incidence of *S. lugdunensis* in human disease, which may lead to an underestimation of its clinical relevance and, consequently, its importance in relation to implant-related osteomyelitis.

Although the pathogenic potentials of *P. acnes* and *S. lugdunensis*, especially in relation to medical device infections, are being increasingly recognized, there has been a limited number of preclinical experimental studies investigating the ability of *P. acnes* or *S. lugdunensis* to cause implant-related osteomyelitis. Therefore, the purpose of this study was to observe the effects of *P. acnes* and *S. lugdunensis* in an established rabbit model (26) of implant-related osteomyelitis, in the absence of implant material wear debris, and characterize the resultant infections with respect to histological and microbiological outcomes.

MATERIALS AND METHODS

Ethics statement. The animal study was approved by the ethics committee of the Canton Grisons in Switzerland (approval no. 06/2008). The

TABLE 1 Primers used in this study

Target	Gene/locus tag	Primer name	Sequence	Reference
16S rRNA gene		fD1	CCGAATTCGTCGACAACAGAGTTTGATCCTGGCTCAG	60
		rP2	CCCGGGATCCAAGCTTACGGCTACCTTGTTACGACTT	60
Von Willebrand factor	*vwbl*	stlu_vwbl_F	TGGCGGGATGATTTGGACGGG	61
		stlu_vwbl_R	TCGCCTTCTTGCCCTGATGGT	61
Fibronectin binding	*fbn*	F1	GGTAATCAGTCATTCGAG	62
		R1	TGGCACACTGTCGAAGTC	62
	fbl	fbl_check_F	CGTATTATCCCAAGTAGCAACC	61
		fbl_check_R	CTTCATCGATTGTCCCAGTAGC	61
	fbpA	FbpA_F	GAGATTACTGGACAACAAACG	61
		FbpA_R	GTATTGTGACGTCGTTTCCTG	61
Hemolytic peptides	*slush*	slush_donvito_F	TTTCGTCTTTGCACACACATTTCCA	61
		slush_donvito_R	ACAGCACAAAGCCTTAACTATCTCA	61
Tannase A	*tanA*	tanA-F	AGCATGGGCAATAACAGCAGTAA	63
		tanA-R	GCTGCGCCAATTTGTTCTAAATAT	63
Beta-hemolysin	SLGD_00006	betahemolysin_F	TGGTCAAGGTACAGAAGGTTGGCA	61
		betahemolysin_R	TATCCCAACTATACGCGTTGCCCT	61
Intercellular adhesion gene A	*icaA*	ICAF	GATGGAAGTTCTGATAATAC	64
		ICAR	CCTCTGTCTGGGCTTGACC	64

animal care and use protocol used for this study adheres to Swiss animal protection laws and its regulations. The bacterial isolates used in this study were obtained from adult patients who provided informed written consent to participate in a clinical study, which was approved by the Faculty of Medicine Research Ethics Committee at Queen's University, Belfast, Northern Ireland. The *P. acnes* isolate was obtained as part of approval no. Ref53/99, and the *S. lugdunensis* isolate was obtained as part of approval no. Ref86/01.

Bacterial isolates. The *P. acnes* strain LED2 was isolated after ultrasound treatment of a retrieved prosthetic hip joint, which was removed at Musgrave Park Hospital, Belfast, Northern Ireland, due to a supposed aseptic joint failure. A bacterial biofilm was also detected in the sonicate fluid by immunofluorescence microscopy (IFM) after labeling with a *P. acnes*-specific antibody, as previously described (11). The *S. lugdunensis* strain 010729 was isolated from an intramedullary (IM) nail-fixed tibial fracture at the Royal Victoria Hospital, Belfast, Northern Ireland. Although the fracture had united, the patient reported ankle pain. *S. lugdunensis* was also isolated from the nail plug and locking screws. Bacterial stock cultures were stored at −80°C in 20% (vol/vol) glycerol using the cryoprotectant bead (Protect) system. *P. acnes* LED2 was grown anaerobically from stock cultures on anaerobic blood agar (ABA) (Oxoid) in a GasPak EZ system with anaerobic sachets (BD Diagnostics, Allschwil, Switzerland). Broth culture of LED2 was performed in proteose peptone yeast (PPY) broth (Oxoid, Basel, Switzerland). Immediately before use, 2 ml of 3.75% (wt/vol) L-cysteine (Sigma-Aldrich, Buchs, Switzerland) and 2 ml of sodium bicarbonate (Sigma-Aldrich) were added to 100 ml of the PPY medium to maintain a reducing environment. *S. lugdunensis* 010729 was cultured on tryptic soy agar (TSA) (Oxoid) or in tryptic soy broth (TSB) (Oxoid) in ambient air at 37°C.

Molecular analyses. Genomic DNA was prepared from single colonies using the Wizard Genomic DNA preparation kit (Promega, Dübendorf, Switzerland), according to the manufacturer's protocol. The primers used for PCR amplification are listed in Table 1. PCR amplification was carried out using an Eppendorf Mastercycler gradient thermal cycler (Vaudaux-Eppendorf, Basel, Switzerland) in a total volume of 12.5 μl containing 10× PCR buffer (Invitrogen, Zug, Switzerland), 5 mM deoxynucleoside triphosphate (dNTP) mix (Promega), 50 pmol of each primer (Microsynth, Balgach, Switzerland), 1 unit of *Taq* DNA polymerase (Invitrogen), and 10 to 50 ng template DNA. The products were separated by electrophoresis on 1% (wt/vol) agarose (Sigma-Aldrich) gels, stained with RedSafe nucleic acid staining solution (iNtRON Biotechnology, Basel,

Switzerland), visualized with UV light, and imaged using a GelDoc XR image analysis station (Bio-Rad, Reinach, Switzerland). The product sizes were estimated using BenchTop 100-bp and 1-kb DNA ladders (Promega) as molecular size markers. The PCR products were purified for sequencing using the PureLink quick gel extraction and PCR purification combo kit (Invitrogen), according to the manufacturer's protocol.

Nucleotide sequencing. Automated sequencing was performed at Microsynth AG (Balgach, Switzerland) on an Applied Biosystems ABI 3730xl sequence analyzer 5.2 using the ABI BigDye system version 3.1. The sequences were compared with known sequences using BLAST (http://blast.ncbi.nlm.nih.gov).

***In vitro* adhesion and biofilm formation.** *In vitro* adhesion of the bacteria to a range of orthopedic metals was measured using the preoperative contamination model of Rochford et al. (27). The metals used were electropolished stainless steel (SS), standard microrough titanium-aluminum-niobium (NS), and electropolished titanium-aluminum-niobium (NE). The adhesion studies were performed in phosphate-buffered saline (PBS) for *S. lugdunensis* and PBS supplemented with 0.05% (vol/vol) L-cysteine for *P. acnes*. Briefly, the bacterial suspension was adjusted to an optical density at 600 nm of 0.5 and diluted 10-fold to give a 1-liter suspension at an approximate density of 1×10^7 CFU per ml; this value was confirmed for each experiment by total viable counts (TVCs). Triplicate 13-mm discs of the test materials were placed into the adhesion chamber, and the liquid was stirred at 125 rpm for 2.5 h at 37°C to measure initial adhesion. The sample discs were retrieved from the chamber and placed in sterile glass bottles containing 5 ml of PBS. The discs were then ultrasonicated for 3 min using an ultrasonic water bath (Bandelin, Germany) operating at 40 kHz, followed by vortex mixing for 20 s to remove the adherent bacteria. The TVCs of the removed bacteria were carried out by serial dilution and plating on blood agar (BA) (Oxoid) or ABA, and these were incubated aerobically for 2 days or anaerobically for 14 days to detect *P. acnes* or *S. lugdunensis*, respectively. Biofilm formation was measured by the method of Stepanović et al. (28). For *S. lugdunensis* 010729, biofilm formation was measured after 24 h of incubation in TSB supplemented with 1% (wt/vol) glucose (Sigma-Aldrich), as recommended by the Stepanović protocol, to ensure reproducible results for other staphylococci. For LED2, biofilm formation was measured after 7 days of incubation in PPY broth supplemented with L-cysteine and sodium bicarbonate, as described above.

***In vivo* animal model.** Custom-made IM nails composed of SS (ISO 5832-1), which were 2.5 mm in diameter and 85 mm in length, were used.

Prior to implantation, all IM nails were washed twice in 70% (vol/vol) ethanol, followed by two periods of sonication in deionized water using an ultrasonic water bath operating at 40 Hz for 15 min. Each nail was then packaged individually and steam sterilized at 121°C for 20 min. Skeletally mature specific-pathogen-free female New Zealand white rabbits (Charles River Laboratories, Sulzfeld, Germany) were used in this study. Each rabbit was assessed by a veterinarian and determined to be healthy prior to inclusion in the study.

Prior to surgery, each rabbit was screened to determine whether the IM nail would be accommodated within the tibia. Under general anesthesia and using aseptic surgical techniques, the patellar ligament of the left tibia was divided and the anterior part of the tibia plateau exposed. The medullary cavity was opened with a 3.5-mm drill bit and evacuated with a 3.0-mm-diameter suction device. Using a catheter, the distal two-thirds of the medullary canal was inoculated with 50 μl of bacterial suspension in 25% (vol/vol) quarter-strength Ringer's solution (QSRS). The bacterial inocula were added to the implant site within 15 min of preparation. The implant was immediately inserted without hammering and the insertion site sealed with a water-soluble alkylene copolymer hemostasis material (Ostene; Ceremed, Inc. CA, USA). The patellar ligament and skin were closed in a routine manner. To minimize variability, the same surgeon operated on all rabbits.

The *P. acnes* inoculum for the animal study was prepared by subculturing a single colony of freshly grown LED2 from ABA into 50 ml PPY broth. The culture was incubated anaerobically for 16 h at 37°C. Immediately prior to surgery, an aliquot was taken and centrifuged at 2,500 rpm for 10 min, and the resulting pellet was resuspended in prereduced QSRS containing the reducing agent L-cysteine (0.05% [vol/vol]). The inoculum density was adjusted to a target of 3×10^7 CFU/50 μl based on an optical density at 600 nm of 0.5. For the *S. lugdunensis* inoculum, one colony was taken from a young (<24 h) TSA culture and inoculated into 20 ml prewarmed TSB. The culture was incubated for 2 h in a shaking water bath at 37°C and 100 rpm. Prior to each surgery, an aliquot was taken and centrifuged at 2,500 rpm for 10 min, resuspended in QSRS, and similarly adjusted to a target density at 600 nm of 0.6, approximately 3×10^7 CFU/50 μl.

A quantitative culture of each inoculum was performed immediately after preparation to determine the exact number of bacteria given to each animal. Serial 10-fold dilutions of the bacterial culture were performed in QSRS and plated onto BA for 24 h (*S. lugdunensis*) or ABA plates for 14 days (*P. acnes*).

Observation and euthanasia. Upon completion of the surgical procedure, baseline radiographs were taken and the rabbits were returned to their individual hutches and monitored for 4 weeks. Each animal was monitored continuously throughout the observation period for signs of systemic infection. No antibiotics were administered to any animal during this study. Daily evaluations of attitude, appetite, and surgical incisions were carried out, while weight and body temperature were recorded weekly. Blood samples were collected preoperatively and weekly thereafter to determine the white blood cell (WBC) count (Vet abc; scil Animal care, Viernheim, Germany). Animal exclusion criteria were set at a weight loss of >10% of the initial body weight within 2 weeks, local infection with severe lameness, persistent swelling and discharge, or signs of systemic infection, such as fever, depression, and anorexia. After 28 days, each animal was humanely euthanized. Pilot surgeries were performed, whereby similar implants were placed, without any inoculation, in two animals. The weights, WBC counts, and histology images of these uninoculated animals were included for comparison.

Postinfection bacteriological analysis. All rabbits receiving an inoculum of either *P. acnes* or *S. lugdunensis* were processed for bacteriological analysis. After euthanasia, the skin was removed from the left leg and wiped down with 70% (vol/vol) ethanol. Swabs were taken from the tibial plateau at the point of insertion of the nail and streaked across BA plates. The tibia was then cut using an oscillating saw to expose the most distal end of the nail. The nail was removed through the distal end of the tibia

and submerged in 6 ml of sterile QSRS, gently agitated for 20 s to remove loosely adherent bacteria, and then transferred to a second bottle of sterile QSRS. The nail was then vortexed for 30 s and subsequently placed in a sonicating water bath operating at a frequency of 40 kHz for 3 min before a final vortex for 30 s. The sonicates were immediately serially diluted in sterile QSRS and 200-μl aliquots spread onto TSA, BA, and ABA plates for quantitative bacterial culture. The tibia was then cut just below the most proximal point previously occupied by the IM nail and the proximal portion fixed for histological processing as described below. A 2-cm section was also removed from the distal end of the tibia for histology. The remainder of the bone that previously surrounded the IM nail was then homogenized in 15 ml QSRS with or without L-cysteine, as appropriate, using a Polytron PT 3100 homogenizer (Kinematica AG, Switzerland). Serially 10-fold diluted and duplicate 200-μl aliquots of the bone homogenate were added to TSA, BA, and ABA plates for incubation. All TSA and BA plates were incubated at 37°C aerobically, and the ABA plates incubated anaerobically, and the results were recorded at 24 h and reexamined after 48 h for *S. lugdunensis*- and 14 days for *P. acnes*-inoculated rabbits. In both groups, aerobic and anaerobic cultures was performed to ensure no secondary infection was present. The lower limit of detection of the bone samples was 75 CFU per bone fragment and 30 CFU for the IM nail. To be considered infected, either the bone or the IM nail was required to yield at least five colonies on both agar plates of the undiluted suspension. All bacterial growth was identified using the Remel RapID ANA II and the RapID Staph Plus system test kits, performed according to the manufacturer's protocols (Remel, Switzerland).

Histology. The proximal and distal tibiae were fixed in 70% (vol/vol) methanol and subsequently decalcified with EDTA. Decalcified blocks were trimmed to include the entry point of the nail and the nail cavity and embedded in paraffin. Six-micrometer sections were cut and stained with hematoxylin and eosin for histomorphological scoring. Adjacent or nearby sections were stained with a modified Brown and Brenn stain to visualize the bacteria.

The regions of interest for histological scoring were the articular surface, entry site and tract of the nail, the medullary canal, cortical bone, and periosteum. Representative sections were graded by a histopathologist, who was blind to the rabbit treatments, for severity and characterization of the infection.

Electron microscopy was performed on representative sections to identify the location of the bacteria within the tissues. The sections were deparaffinized, sputter coated with gold palladium and then imaged using a Hitachi S-4700 scanning electron microscope (SEM). Images were taken in the secondary electron mode with an accelerating voltage of 5 kV.

RESULTS

Strain characterization and adhesion properties. *P. acnes* strain LED2 belongs to the type IB sequence type 5 (ST5) lineage (clonal complex 5 [CC5]), based on multilocus sequence typing (MLST) analysis of six core housekeeping genes and two putative virulence genes (16, 29, 30). It is hemolytic on horse and sheep ABA, has a demonstrable cohemolytic CAMP reaction, and expresses an abundance of the CAMP factor 1 protein as detected by SDS-PAGE and immunoblotting (31). In keeping with its identification as a type IB strain, it does not react with monoclonal antibodies specific for the phase-variable dermatan sulfate-binding adhesins present on the surface of type IA and IC isolates (32). *S. lugdunensis* 010729 is positive for the *vwbl* gene, which encodes the Von Willebrand factor, and fibronectin-binding proteins encoded by the *fbn*, *fbl*, and *fbpA* genes. Genes encoding beta-hemolysin and hemolytic peptides were also detected by PCR amplification. The intercellular adhesion gene *icaA* was also present.

In the bacterial adhesion assay, *S. lugdunensis* 010729 adhered in similar amounts to all of the metals tested (analysis of variance [ANOVA], $P = 0.790$), though the variation among the results
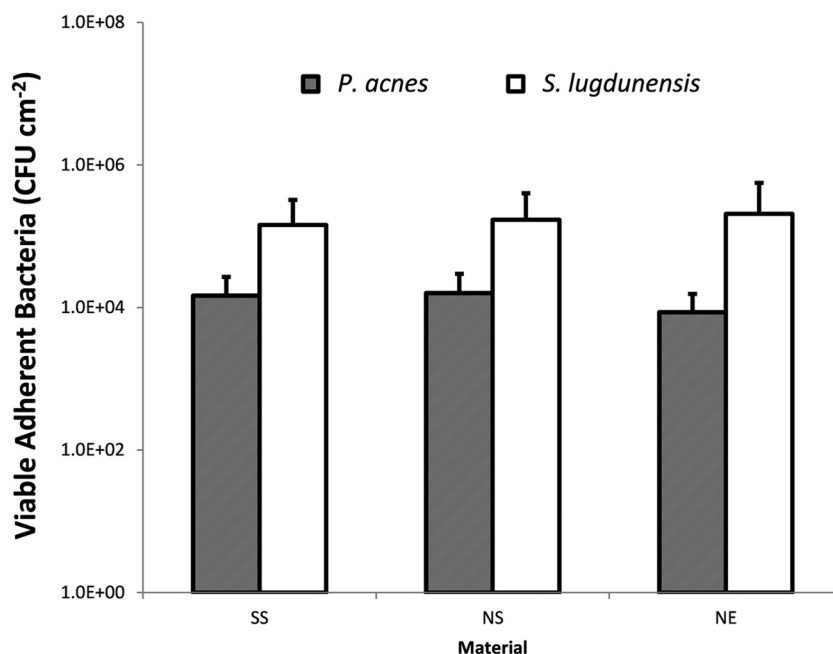
FIG 1 Total viable counts of bacteria retrieved from stainless steel (SS), electropolished titanium-aluminum-niobium (NE), and standard microrough titanium-aluminum-niobium (NS) after incubation *in vitro* for 2.5 h with *P. acnes* LED2 and *S. lugdunensis* 010729. Error bars represent standard deviations.

was high (Fig. 1). The number of viable *P. acnes* cells retrieved from the materials was less than that of *S. lugdunensis*, although the amounts in the initial inocula were equivalent between groups. In addition, there were significantly fewer *P. acnes* adhering to NE than to SS and NS (ANOVA $P = 0.050$). The ability to form a biofilm *in vitro* was determined for LED2 and 010729 using the crystal violet staining method and classification scheme of Stepanović et al. (28). Under these conditions, *S. lugdunensis* produced a moderate biofilm within 24 h, with an optical density (A_{600}) and standard deviation (SD) of 0.12 ± 0.01, while *P. acnes* produced a moderate biofilm with A_{600} and SD of 0.10 ± 0.01 at day 7; however, only weak biofilm ($A_{600} < 0.05$) formation was identified prior to day 7.

Surgery and observation. Postoperative radiographs showed good placement of the IM nail without any observable fractures. All rabbits tolerated the surgical procedure, and no animals were excluded from the study due to perioperative complications or postoperative sepsis. Posteuthanasia radiographs showed there was no migration of the implant, and no radiographic signs of severe osteolysis were observed (Fig. 2). Table 2 shows weight and WBC count values for *P. acnes*- and *S. lugdunensis*-infected animals and uninoculated rabbits throughout the study period. The uninoculated rabbits displayed a minor peak in WBC count and weight loss in the first postoperative week, both of which had returned to preoperative values prior to completion of the observation period, with overall weight gain observed by the completion of the study. The *P. acnes*-infected rabbits displayed minor weight loss in the first postoperative days, followed by full recovery and some weight gain, though less than that in the uninoculated animals. The WBC count also showed a minor spike in the first weeks, which was greater and more persistent than that observed in uninoculated animals. However, the WBC count returned to normal after the 4-week observation period. The *S. lugdunensis*-infected rabbits displayed, on average, a greater weight

loss in the first 2 weeks, and by the end of the study, they had not gained any weight. The WBC count also showed a more pronounced and persistent elevation than that displayed by the *P. acnes*-infected animals, although the baseline WBC count was greater in the *S. lugdunensis*-infected group.

Bacteriological outcomes. The average intraoperative bacterial inoculum given to the rabbits that received *P acnes* LED2 was 1.67×10^7 CFU. Upon completion of the observation period, only 1/6 *P. acnes*-inoculated animals were culture positive from the joint swab. The bone cultures were positive for all six *P. acnes*-inoculated rabbits. Quantitative bacteriological analysis after sonication of the implant showed that all six *P. acnes*-inoculated animals were positive for biofilm on the IM nail. The TVC values of biofilm (sonication fluid and loosely adherent biofilm) and bone cultures (per gram) is shown in Fig. 3. On average, the total CFU counts cultured from the culture-positive bone samples and implants were 2.6×10^5 CFU and 3.3×10^6 CFU, respectively. In all cases, the microorganism cultured from the bone or the implants of the LED2-inoculated animals was confirmed to be *P. acnes* using Remel RapID diagnostic kits. IFM analysis with a monoclonal antibody (QUBPa3) (33) to *P. acnes* also confirmed the presence of the bacterium in sonicate samples (data not shown). No other bacterial species, based on colony morphology, were identified in any of the samples from these rabbits.

The average intraoperative bacterial inoculum given to the rabbits that received *S. lugdunensis* 010729 was 2.49×10^7 CFU. At the completion of the 4-week observation period, 4/6 *S. lugdunensis*-inoculated rabbits were culture positive from the joint space swab. The bone cultures were also positive for the same rabbits and negative in the remaining two rabbits. No bacteria were isolated from animals recorded as culture negative. Quantitative bacteriological analysis after sonication of the implant showed that only 2/6 rabbits receiving the *S. lugdunensis* inoculum were positive for biofilm on the IM nail, both of whom were also culture positive from the bone. The TVCs of
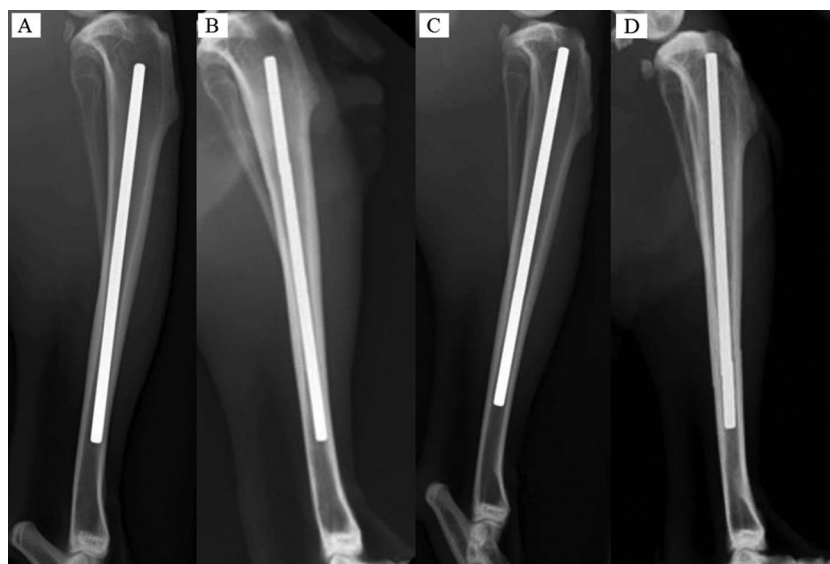
FIG 2 Representative postoperative and postmortem radiographs of rabbit tibiae. (A) Postoperative radiograph of a rabbit that received a *P. acnes* inoculum; (B) postmortem radiograph of the same animal after 28 days. (C) Similar postoperative radiograph for a rabbit receiving an *S. lugdunensis* inoculum; (D) postmortem radiograph from the same animal taken after 28 days. No radiographically evident signs of infection were observed for either bacterial species.

the biofilm (sonication fluid and loosely adherent biofilm) and bone cultures (per gram) of each animal are shown in Fig. 4. On average, the total CFU counts cultured from the positive bone samples and implants were 5.1×10^6 CFU and 1.3×10^6 CFU, respectively. In all cases, the microorganism cultured from the bone or the implant of the *S. lugdunensis*-inoculated animals was confirmed to be *S. lugdunensis* using the Remel diagnostic kit. Sequence analysis of the 16S rRNA gene PCR fragment revealed 100% identity to the sequence of *S. lugdunensis* present in GenBank under accession no. N920143. As with *P. acnes*, IFM with a monoclonal antibody (QUBSe1) to staphylococci also confirmed the presence of the bacterium in sonicate samples (data not shown). No other bacterial species, based on colony morphology, were identified in any of the samples from these rabbits. All samples from the uninoculated rabbits were negative from the joint swab, bone samples, and sonicated nail sample.

Histology. Characteristic features of osteomyelitis, such as micro- and macroabscesses, and the increased presence of neutro-

phils and other inflammatory cells were observed to various degrees in all six *P. acnes*-infected rabbits (Table 3). Focal inflammatory changes were seen in the subarticular region; however, the presence of fibrocartilage indicated the ulcerations were healing, and no subarticular macroabscesses were identified (Fig. 5). A higher-grade osteomyelitis was observed adjacent to the implant, where diffuse inflammation was seen, with some preservation of the microarchitecture (Fig. 6). These pathologies were not observed in this model as a result of implantation of the IM alone (Fig. 5 and 6). After Brown and Brenn staining, all specimens revealed the presence of bacteria, which primarily localized in small clusters located between adipocytes in the distal medullary cavity, which was confirmed by SEM imaging (Fig. 7).

The histological features of the *S. lugdunensis* infection were consistent with pyogenic osteomyelitis and septic arthritis, as summarized in Table 3. Focal inflammatory changes were seen in all animals with either micro- or macroabscesses in the subarticular region (Fig. 5 and 6). There was evidence of septic arthritis in all

TABLE 2 Change in body weight and white cell count over time

Results by inoculation type	Data by time in relation to surgery (mean ±SD [range])					
	Preoperative	3 days	7 days	14 days	21 days	28 days
Uninoculated						
Wt change (kg)[a]	0.00	0.044 ± 0.06	−0.06 ± 0.05	0.12 ± 0.08	0.12 ± 0.09	0.32 ± 0.08
WBC count ($\times 10^3$/mm^3)	5.11 ± 1.16	6.95 ± 1.56	7.12 ± 1.32	5.77 ± 1.01	5.82 ± 1.43	6.00 ± 1.22
P. acnes LED2						
Wt change (kg)	0.00	−0.15 ± 0.11 (−0.34 to −0.01)	−0.11 ± 0.10 (−0.24 to −0.01)	0.15 ± 0.09 (0.08 to 0.33)	−0.07 ± 0.11 (−0.22 to 0.09)	0.17 ± 0.11 (−0.01 to 0.30)
WBC count ($\times 10^3$/mm^3)	3.82 ± 0.67 (3.24 to 5.14)	8.10 ± 1.40 (6.80 to 10.66)	8.16 ± 1.16 (7.01 to 9.78)	7.07 ± 1.58 (5.77 to 10.18)	6.83 ± 0.15 (6.72 to 6.93)	3.86 ± 0.79 (3.29 to 4.42)
S. lugdunensis 010729						
Wt change (kg)	0.00	−0.27 ± 0.11 (−0.43 to −0.15)	−0.23 ± 0.03 (−0.26 to −0.17)	−0.08 ± 0.10 (−0.26 to −0.03)	−0.08 ± 0.05 (−0.17 to −0.03)	−0.01 ± 0.05 (−0.08 to 0.06)
WBC count ($\times 10^3$/mm^3)	4.70 ± 1.22 (3.43 to 6.49)	9.26 ± 3.51 (7.06 to 16.27)	10.56 ± 1.98 (7.10 to 12.21)	8.83 ± 1.49 (7.36 to 11.61)	7.42 ± 1.15 (6.60 to 8.23)	4.91 ± 1.24 (4.03 to 5.79)

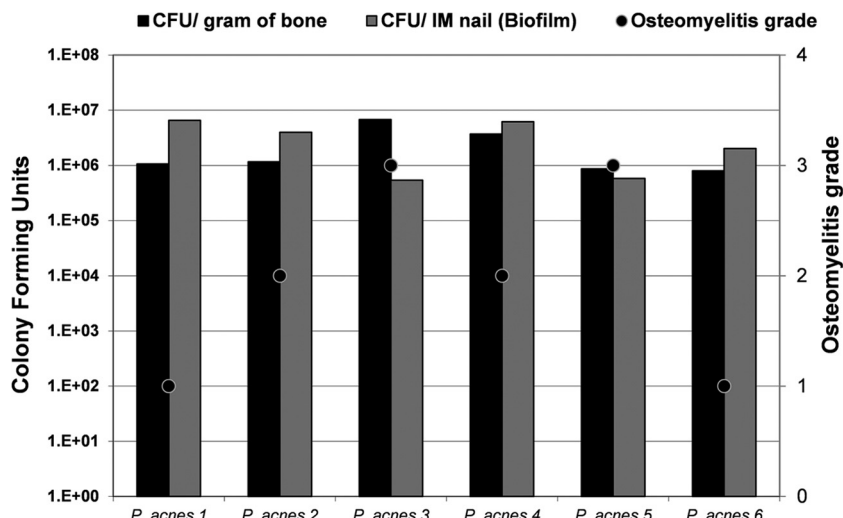[a] Change in body weight from preoperative weight.

FIG 3 Quantitative culture of *P. acnes* LED2 from the bone and implant of each rabbit.

six rabbits, with subarticular abscesses communicating with the adjoining joint in four of the animals. These pathologies were not observed in this model as a result of implantation of the IM alone (Fig. 5 and 6). After Brown and Brenn staining, bacteria were seen in all specimens examined (Fig. 7), including the two culture-negative animals. Bacteria were seen on the edges of the subarticular abscesses, while none or few were identified within the abscesses themselves. Small clusters were also located between adipocytes in the medullary cavity adjacent to activated erythropoietic and myelopoietic cells, indicative of early osteomyelitis. Some bacterial cells also appeared to have been phagocytosed by inflammatory cells in the bone marrow, although the viability of these bacteria was not determined (shown in Fig. 7). SEM analysis showed the scattered presence of *S. lugdunensis* throughout the tissue (Fig. 7), although an intracellular localization of *S. lugdunensis* could not be confirmed by SEM.

DISCUSSION

Historically, microorganisms, such as *P. acnes* and CoNS, have been considered contaminants from the skin rather than causative agents of osteomyelitis (3–5). Reports from the Patrick laboratory at Queen's University Belfast in the late 1990s (11, 34) revealed the isolation and detection of these microbes in significant numbers from aseptically loosened failed implants by the use of ultrasound to dislodge adherent biofilms. These data suggested that these apparently low virulence commensal microorganisms might in fact be important pathogens capable of causing significant numbers of implant-related bone infections, leading to osteolysis and implant failure. Subsequent studies have supported these findings (10, 35–38), and further work at Queen's University Belfast (QUB) also provided evidence of colonization of the bone adjacent to the implant (39). Despite this, the question of whether these bacteria are passive bystanders or drivers of prosthetic joint failure has been an ongoing subject of debate, with wear debris arising from implant materials still considered to be a major driver of implant failure (6).

While a large amount of research has been carried out to understand the pathogenic nature of *S. aureus* and *Staphylococcus epidermidis*, there is only limited information available for *P. acnes*
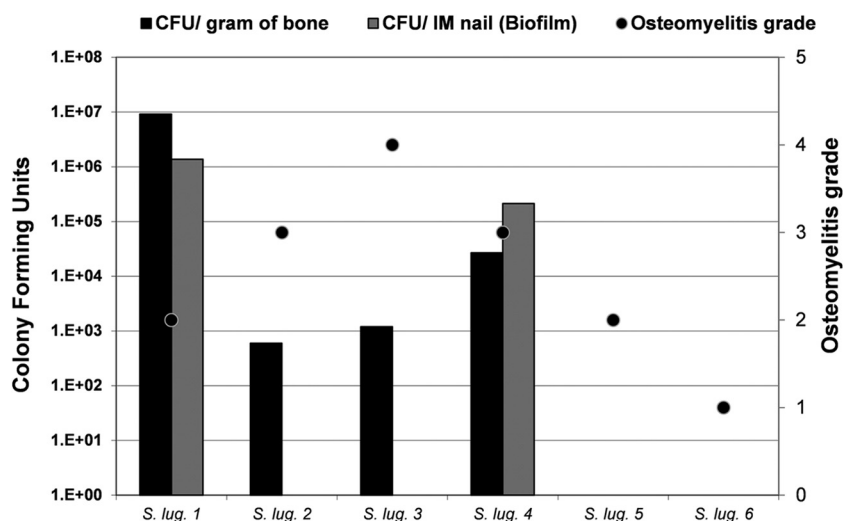

FIG 4 Quantitative culture of *S. lugdunensis* 010729 from the bone and implant of each rabbit (*S. lug. 1* through *S. lug. 6*).

TABLE 3 Summary of the histological findings associated with *P. acnes* LED2 and *S. lugdunensis* 010729 infection

Location and histological feature	Grade or score	No. of animals (of 6) for each category with:			
		S. lugdunensis 010729		*P. acnes* LED2	
		Subarticular	Medullary	Subarticular	Medullary
Articular cartilage					
Presence of ulceration	Yes/no	4	NA[a]	1	NA
Presence of fibrocartilage, indicating healed ulceration	Yes/no	1	NA	1	NA
Presence of inflammatory cells or bacteria in the ligament, indicating septic arthritis	Yes/no	6	NA	1	NA
Subarticular region, entry tract, and medullary cavity					
Diffuse increase in the cellularity of the marrow with near normal preservation of the marrow architecture (fat cells and precursors)	Grade 1 myelitis	1	2	2	0
Presence of ≤5 microabscesses with or without a diffuse increase in cellularity similar to grade 1	Grade 2 myelitis	2	0	2	1
Presence of >5 microabscesses with or without a diffuse increase in cellularity similar to grade 1	Grade 3 myelitis	2	3	2	1
Presence of macroabscesses defined as collection of neutrophils with a fibrous capsule OR a localized gross increase in cellularity	Grade 4 myelitis	1	1	0	1
Diffuse gross increase in neutrophils and inflammatory cells in the entire medullary canal inclusive of the periphery and center	Grade 5 myelitis	0	0	0	3
Presence of necrotic bone or sequestrum	Yes/no	1	2	0	0
Presence of fibrosis	Yes/no	6	6	6	6
Cortical bone					
Increase in the size of the lacunae with neutrophils	Yes/no	NA	2	NA	2
Presence of hyaline degeneration of vessels	Yes/no	NA	0	NA	0
Presence of vascular neutrophilia	Yes/no	NA	3	NA	1
Presence of empty lacunae	Yes/no	NA	5	NA	1
Fibrosis	Yes/no	NA	6	NA	4
Presence of necrotic bone or sequestrum	Yes/no	NA	3	NA	0
Inflammatory cells under the periosteum/subperiosteal abscess	Yes/no	NA	2	NA	3

[a] NA, not applicable.

and *S. lugdunensis* and even fewer studies focusing on preclinical *in vivo* models of infection (40–43). This lack of study also extends to the appropriateness of antimicrobial therapies for these microorganisms, the serological response to their infection, and the role of microbial virulence factors on the progression of infection. To address this issue, we established an experimental implant-related osteomyelitis model based on one described for *S. aureus* (26), for the study of *P. acnes*- and *S. lugdunensis*-related infections. The model incorporates implanted IM nails, which, as with all indwelling biomaterials, provide enhanced colonization opportunities for professional pathogens and opportunistic pathogens alike. For

our study, we used a strain of *P. acnes* that was isolated from sonicate prepared from a failed prosthetic hip joint. This isolate had been previously characterized by MLST, which revealed that it belonged to the ST5 lineage within the type IB phylogenetic group (29). Isolates from this phylogroup are associated with healthy skin and are rarely recovered from acne vulgaris lesions. They have, however, been associated with soft tissue and medical device-related infections, although their exact clinical importance in these cases has remained unclear (16, 29). To date, a total of 13 distinct type IB STs have been described in the *P. acnes* MLST database (http://pubmlst.org/pacnes/) based on the analysis of 69
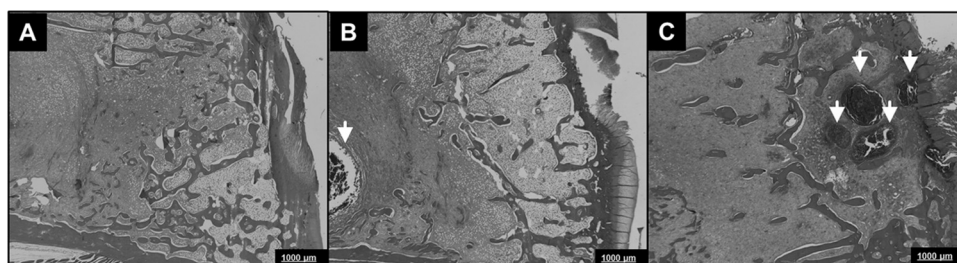

FIG 5 Micrographs illustrating histological analysis of the point of entry of the nail and subarticular region for uninfected (A), *P. acnes* LED2-infected (B), and *S. lugdunensis* 010729-infected (C) rabbits. (A) The entry point has healed completely and no subarticular abscesses are observed. (B) Healing of the point of entry of the nail is also seen, and no signs of subarticular abscess formation were observed. Increased numbers of inflammatory cells were present deep in the medullary cavity adjacent to the implant site (arrow). (C) Macroabscesses were observed just below the articular surface (arrows) (grade 4). Hematoxylin and eosin staining was used.
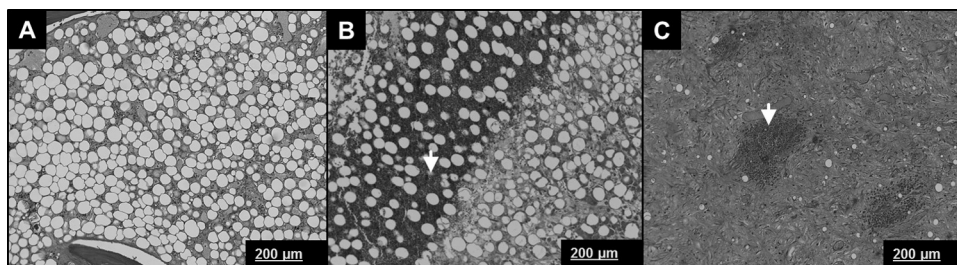
FIG 6 Micrographs illustrating histological analysis of the medullary region of uninfected (A), *P. acnes* LED2-infected (B), and *S. lugdunensis* 010729-infected (C) rabbits. (A) The medullary region displays normal physiology with abundant univacuolar adipocytes and the lack of cellular infiltration. (B) A diffuse marked increase in cellularity indicative of grade 3 osteomyelitis is seen (white arrow). (C) Focal inflammatory changes, such as microabscesses, are seen in the medullary region, with a marked decrease in adipocytes (white arrow). Hematoxylin and eosin staining was used.

type IB isolates, of which 11 belong to a single CC, with ST5 as the founder genotype (CC5) (bootstrap value, 99%), while two isolates are singletons (ST12 and ST51). As expected for a founding genotype, the ST5 clonal lineage is highly prevalent in the human population and is globally disseminated. *P. acnes* contains an expanded family of five CAMP factor homologues that appear to have arisen primarily as a result of horizontal gene transfer (HGT), as judged by previously described colocalization and sequence similarity criteria (16). Previous studies with five type IB *P. acnes* isolates (all subsequently identified as belonging to the ST5 lineage by MLST) demonstrated abundant production of the CAMP factor 1 protein in a comparison with strains from the type IA division; the secretion of large quantities of CAMP 1 was also observed with isolates from the large type II clade (29, 31). Cur-

rently, the exact role played by CAMP 1 and the other CAMP factor homologues is unclear, but they may play an important role in the survival of *P. acnes* within the human host as well as contributing to a pathogenic lifestyle (16). Recently, an MLST scheme and database for *S. lugdunensis* were described based on the analysis of seven core housekeeping genes (44). A clonal population structure with limited sequence diversity was revealed, and isolates recovered from hematogenic infections (blood or osteoarticular isolates) or from skin and soft tissue infections were not found to cluster in separate lineages. Currently, we do not have MLST data for *S. lugdunensis* 010729, but we are now analyzing the strain by whole-genome sequencing, which will facilitate the immediate assignment of an ST and CC when data for each of the MLST loci are complete.
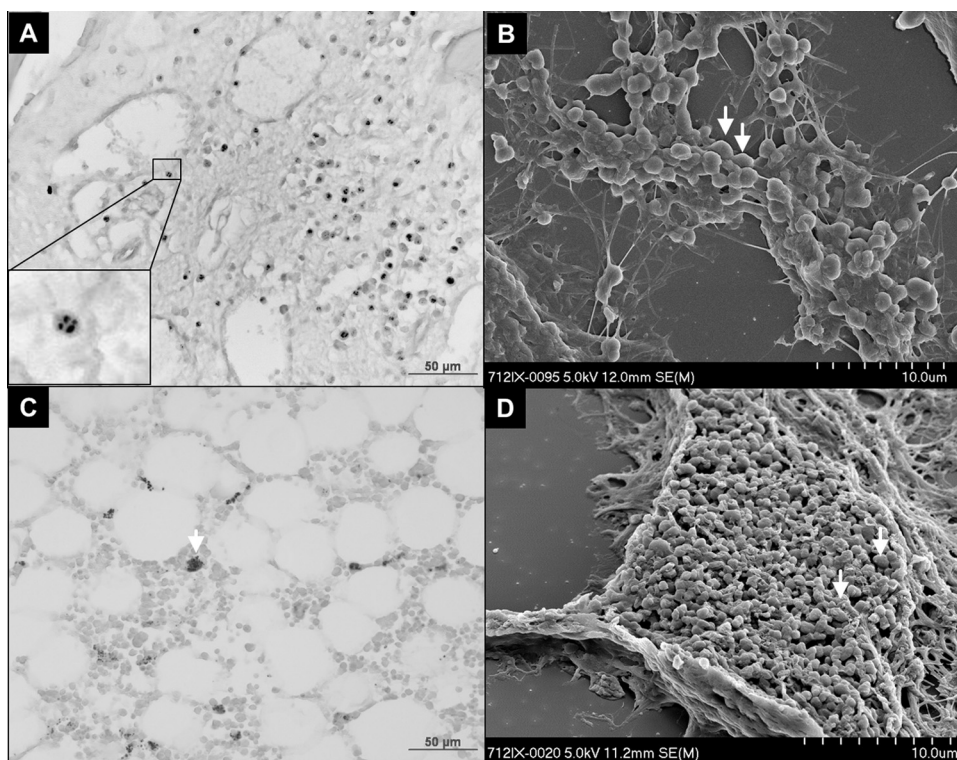

FIG 7 Micrograph illustrating the localization of bacteria within infected animals. *S. lugdunensis* was primarily associated with abscesses (A), and an intracellular localization of *S. lugdunensis* was also observed (modified Brown and Brenn staining). (B) Scanning electron micrograph of bacterial cells in medullary area (arrows). (C) *P. acnes* cells were arranged in clusters (arrow) adjacent to adipocytes in the medullary cavity. (D) Scanning electron micrograph of bacterial cells in the medullary area. Note the pleomorphic rod morphology characteristic of *P. acnes* (arrows).

The experimental model used here requires the direct artificial inoculation of bacteria into the surgical field, which it must be noted will exceed the number of bacteria likely to contaminate a surgical wound during a primary elective procedure. However, if a failed prosthetic joint with a misdiagnosis of aseptic loosening is removed and a new sterile device is placed in the underlying infected site, it is very possible that higher numbers of bacteria will be present, particularly if the adjacent bone has been colonized. The bacterial inoculum we used (3×10^7 CFU) is well within the range of inocula previously applied in other experimental rabbit models of staphylococcal implant-related osteomyelitis (for example, 3×10^6 to 2×10^8 CFU [26, 45, 46]). Upon completion of the study, the total CFU counts recovered from both *P. acnes*- and *S. lugdunensis*-infected rabbits were quite varied, although the majority of culture-positive samples were between 1×10^6 and 1×10^7 CFU for *P. acnes* and 1×10^3 and 1×10^7 CFU for *S. lugdunensis*. The total numbers of bacteria quantitatively cultured from this study are similar to the numbers of *S. aureus* cultured from the previous model on which our study is based (26). The lower recovery of *S. lugdunensis*, in particular the lack of a consistent biofilm, is an interesting finding further discussed below.

The general histopathological features of osteomyelitis observed in this model included the presence of diffuse, focal, and multifocal inflammation characterized by infiltration of the medullary canal by neutrophils and the presence of subarticular and peri-implant abscesses with surrounding fibrosis. A histopathological scoring system, based upon similar studies using *S. aureus* (47–49), was developed to specifically focus upon the features of implant-related osteomyelitis as it occurs after intramedullary nailing. This scoring system was then used to determine whether there were differences in the characteristics of any infection caused by these two species of bacteria. In animals that underwent surgery but were uninoculated, the entry point of the nail healed uneventfully, and the medullary area displayed a physiological appearance, lacking in increased cellularity or significant fibrosis. A comparatively severe histopathology, characterized by macroabscess formation and septic arthritis, was observed after infection with *S. lugdunensis*. Although *S. aureus*-infected animals were not compared directly in this implant model, the histopathology of the *S. lugdunensis*-inoculated animals was comparable to that seen in a similar animal model using *S. aureus* (48). This is consistent with the association of *S. lugdunensis* with a clinical course more similar in severity to a typical *S. aureus* infection than to that caused by other CoNS (17). A complete-genome sequence of *S. lugdunensis* did not reveal the well-recognized virulence determinants that enable *S. aureus* to cause acute infection, but different strains of *S. lugdunensis* may carry other putative virulence determinant genes gained as a result of HGT (17, 50). Interestingly, the *S. lugdunensis* infection was not significantly associated with biofilm formation, as a biofilm was detected by culture on the IM nail of only 2/6 animals. This is despite *in vitro* biofilm formation by this *S. lugdunensis* isolate on a range of implant materials. However, the *S. lugdunensis* bacterium was observed in all histological sections after 28 days *in vivo*. The histological analysis revealed that *S. lugdunensis* was predominantly found adjacent to abscesses and in many cases appeared intracellularly within phagocytic cells in the abscess tissue. The viability of these intracellular bacteria is not known, but intracellular survival is a feature associated with *S. aureus* and *S. epidermidis* and is entirely in keeping with the intracellular survival of other CoNS (51). The intracellular location of

S. lugdunensis is a potential explanation for the culture-negative animals observed in this study. Non-culture-based detection of staphylococci has also previously been described for culture-negative retrieved failed prostheses and biopsy specimens from human patients with long-bone nonunion of fractures (52). The culture-negative animals may also be due to an unavoidable sampling error, leading to a bacterial presence in the bone sample retained for histology yet absent from the biopsy specimens retained for bacterial culture. What is clear, however, is that the histopathology of the culture-negative *S. lugdunensis*-inoculated animals indicates an active infection in these animals. Further study is required to definitively characterize the natural progression of the infection in this model and determine whether this culture-negative finding indicates a subsidence of the infection.

In the *in vivo* model, *P. acnes* causes an infection characterized by biofilm formation and localized inflammation adjacent to the biofilm and implant. According to the histological scoring, *P. acnes* did not cause septic arthritis, and the entry wound from the insertion of the IM nail was found to be healing with fibrocartilaginous tissue formation. The histological scoring of the medullary area adjacent to the implant and the biofilm was greater than that in the subarticular region, and even greater in severity than the *S. lugdunensis* data. These pathologies are not observed with implantation of the IM alone (Fig. 5 and 6). The *P. acnes* microcolonies were observed primarily adjacent to the adipocytes within the medullary cavity, some of which also showed regions with high-grade osteomyelitis. SEM analysis confirmed microcolony formation (Fig. 7) in the intercellular regions in the bone marrow, and there was no evidence of intracellular localization of *P. acnes* by SEM or light microscopy. The clinical signs, such as weight loss and white blood cell count, were less severe in the *P. acnes*-infected animals than in those infected with *S. lugdunensis*. Uninoculated animals gained more weight than *P. acnes*-infected animals, which supports the view that *P. acnes* causes chronic low-grade infections characterized by subtle clinical signs and symptoms and a significantly different histopathology than that from staphylococcal osteomyelitis.

Overall, both the *in vitro* and *in vivo* evaluations indicated that *P. acnes* differs in many respects to *S. lugdunensis*. Our *in vitro* study revealed that *P. acnes* adhered relatively poorly to a range of implant materials compared to *S. lugdunensis*. *In vitro* formation of biofilm and adhesion to orthopedic materials have been shown for *P. acnes* (31, 53–56), although a correlation between *in vitro* and *in vivo* studies is lacking. Our isolate, LED2, displayed weak biofilm formation *in vitro*, although this is clearly not representative of the clinical situation, or even for our experimental infection. Our *in vivo* data revealed that *P. acnes* formed a biofilm in all the animals examined; in contrast, *S. lugdunensis* appeared to have reduced ability to do so under these conditions. The relationship between biofilm formation and osteomyelitis therefore requires further investigation, particularly in the case of *S. lugdunensis*. Of high importance is the observation that more severe medullary osteomyelitis was observed in *P. acnes*-infected animals compared to those infected with *S. lugdunensis*. The most severe grade of intramedullary osteomyelitis, grade 5, was observed in three rabbits infected with *P. acnes* but in none infected with *S. lugdunensis*. The model used is a nonloaded IM nail without any interlocking bolts. As such, there is no risk of any wear-induced particles or fretting corrosion, and no such particles were observed in any histological section. Furthermore, osteomyelitis was not observed

where the IM was implanted in the absence of either *S. lugdunensis* or *P. acnes*. This indicates that *P. acnes* can cause osteomyelitis in the absence of implant material wear debris and in the absence of overt clinical signs of infection. With regard to *S. lugdunensis*, the model confirms that this is a potentially pathogenic coagulase-negative staphylococcal species and that biofilm formation is not a prerequisite for infection.

These results have important implications in relation to distinguishing between true aseptic joint loosening driven solely by, for example, wear particle-mediated inflammation, and chronic infection-driven loosening, which may also be combined with wear debris involvement. These findings may also have wider implications in relation to the involvement of such bacteria in other conditions, such as dental infection (57) and synovitis-acnes-pustulosis-hyperostosis-osteitis (SAPHO) syndrome (58, 59). It would be interesting to follow the progression of both infections histologically over a longer time period and as it becomes more chronic in nature. It would also be valuable to investigate the effect of these pathogens on pseudarthrosis or delayed healing; however, currently, there is no standardized rabbit model of implant-related osteomyelitis with a fracture. Nevertheless, the model showed that the progression of implant-related osteomyelitis follows a bacterial species-specific course and highlights the potential of *P. acnes* and *S. lugdunensis* to cause significant implant-related osteomyelitis.

Based on the study, we conclude that both *P. acnes* and *S. lugdunensis* are pathogens capable of producing osteomyelitis in a rabbit model but exhibit different pathologies. The infection caused by *S. lugdunensis* was in keeping with a classically virulent microbe, with macroabscess formation and failure to heal entry wounds, but only a maximum grade 4 intramedullary osteomyelitis was observed in a single rabbit, with the remaining rabbits experiencing lower-grade osteomyelitis. Interestingly, the *S. lugdunensis* infection was not always characterized by biofilm formation, even when bacteria were present in the adjacent bone. This result may have important clinical implications with regard to the location and extent of tissue debridement required for implant revision/removal, which commonly centers on implant removal only. In contrast, the infection caused by *P. acnes* was characterized by healing of the entry wound and low morbidity for the animals; however, there was extensive biofilm formation and, most significantly, evidence of grade 5 intramedullary osteomyelitis. This occurred in the absence of implant material wear debris. This experimental study therefore provides strong evidence for a potential key role of *P. acnes* in prosthetic joint infection and fracture nonunion in the absence of signs of classical infection and patient morbidity. *P. acnes* should therefore no longer be dismissed as an insignificant pathogen in the setting of failed retrieved implants; clinical diagnostic practice should be tailored to enable the efficient detection of *P. acnes*. Without this, there is the risk of an incorrect diagnosis of aseptic loosening, and subsequent patient treatment may be misinformed.

ACKNOWLEDGMENTS

REFERENCES

1. **Stoodley P, Nistico L, Johnson S, Lasko LA, Baratz M, Gahlot V, Ehrlich GD, Kathju S.** 2008. Direct demonstration of viable *Staphylococcus aureus* biofilms in an infected total joint arthroplasty. A case report. J. Bone Joint Surg. Am. **90:**1751–1758. http://dx.doi.org/10.2106/JBJS.G.00838.

2. **Trampuz A, Zimmerli W.** 2006. Diagnosis and treatment of infections associated with fracture-fixation devices. Injury **37**(Suppl 2):S59–S66. http://dx.doi.org/10.1016/j.injury.2006.04.010.

3. **Clayton JJ, Baig W, Reynolds GW, Sandoe JAT.** 2006. Endocarditis caused by *Propionibacterium* species: a report of three cases and a review of clinical features and diagnostic difficulties. J. Med. Microbiol. **55:**981–987. http://dx.doi.org/10.1099/jmm.0.46613-0.

4. **Fadel HJ, Patel R, Vetter EA, Baddour LM.** 2011. Clinical significance of a single *Staphylococcus lugdunensis*-positive blood culture. J. Clin. Microbiol. **49:**1697–1699. http://dx.doi.org/10.1128/JCM.02058-10.

5. **Patrick S, McDowell A.** 2013. *Propionibacterium acnes*: an emerging pathogen in biomaterial-associated infection, p 87–105. *In* Moriarty TF, Zaat SAJ, Busscher HJ (ed), Biomaterials associated infection. Springer, New York, NY.

6. **Ollivere B, Wimhurst JA, Clark IM, Donell ST.** 2012. Current concepts in osteolysis. J. Bone Joint Surg. Br. **94:**10–15. http://dx.doi.org/10.1302/0301-620X.94B1.28047.

7. **Costerton JW, Post JC, Ehrlich GD, Hu FZ, Kreft R, Nistico L, Kathju S, Stoodley P, Hall-Stoodley L, Maale G, James G, Sotereanos N, DeMeo P.** 2011. New methods for the detection of orthopedic and other biofilm infections. FEMS Immunol. Med. Microbiol. **61:**133–140. http://dx.doi.org/10.1111/j.1574-695X.2010.00766.x.

8. **Gaillard C, Dupond M, Brisou P, Gaillard T.** 2013. Septic nonunions of lower limb long bones: don't neglect *Propionibacterium acnes*! Int. J. Low Extrem. Wounds. http://dx.doi.org/10.1177/1534734613489990.

9. **Schäfer P, Fink B, Sandow D, Margull A, Berger I, Frommelt L.** 2008. Prolonged bacterial culture to identify late periprosthetic joint infection: a promising strategy. Clin. Infect. Dis. **47:**1403–1409. http://dx.doi.org/10.1086/592973.

10. **Tsai CE, Lee FT, Chang MC, Yu WK, Wang ST, Liu CL.** 2013. Primary cervical osteomyelitis. J. Chin. Med. Assoc. http://dx.doi.org/10.1016/j.jcma.2013.07.011.

11. **Tunney MM, Patrick S, Curran MD, Ramage G, Hanna D, Nixon JR, Gorman SP, Davis RI, Anderson N.** 1999. Detection of prosthetic hip infection at revision arthroplasty by immunofluorescence microscopy and PCR amplification of the bacterial 16S rRNA gene. J. Clin. Microbiol. **37:**3281–3290.

12. **Levy PY, Fenollar F, Stein A, Borrione F, Cohen E, Lebail B, Raoult D.** 2008. *Propionibacterium acnes* postoperative shoulder arthritis: an emerging clinical entity. Clin. Infect. Dis. **46:**1884–1886. http://dx.doi.org/10.1086/588477.

13. **Guío L, Sarriá C, de las Cuevas C, Gamallo C, Duarte J.** 2009. Chronic prosthetic valve endocarditis due to *Propionibacterium acnes*: an unexpected cause of prosthetic valve dysfunction. Rev. Esp. Cardiol. **62:**167–177. http://dx.doi.org/10.1016/S1885-5857(09)71535-X.

14. **Kanafani ZA, Sexton DJ, Pien BC, Varkey J, Basmania C, Kaye KS.** 2009. Postoperative joint infections due to *Propionibacterium* species: a case-control study. Clin. Infect. Dis. **49:**1083–1085. http://dx.doi.org/10.1086/605577.

15. **Viraraghavan R, Jantausch B, Campos J.** 2004. Late-onset central nervous system shunt infections with *Propionibacterium acnes*: diagnosis and management. Clin. Pediatr. (Phila) **43:**393–397. http://dx.doi.org/10.1177/000992280404300413.

16. **McDowell A, Nagy I, Magyari M, Barnard E, Patrick S.** 2013. The opportunistic pathogen *Propionibacterium acnes*: insights into typing, human disease, clonal diversification and CAMP factor evolution. PLoS One **8:**e70897. http://dx.doi.org/10.1371/journal.pone.0070897.

17. **Frank KL, Del Pozo JL, Patel R.** 2008. From clinical microbiology to infection pathogenesis: how daring to be different works for *Staphylococcus lugdunensis*. Clin. Microbiol. Rev. **21:**111–133. http://dx.doi.org/10.1128/CMR.00036-07.

18. **Freney J, Brun Y, Bes M, Meugnier H, Grimont F, Grimont PAD, Nervi**

C, Fleurette J. 1988. *Staphylococcus lugdunensis* sp. nov. and *Staphylococcus schleiferi* sp. nov., two species from human clinical specimens. Int. J. Syst. Bacteriol. **38**:168–172. http://dx.doi.org/10.1099/00207713-38-2 -168.

19. Sampathkumar P, Osmon DR, Cockerill FR, III. 2000. Prosthetic joint infection due to *Staphylococcus lugdunensis*. Mayo Clin. Proc. **75**:511–512. http://dx.doi.org/10.4065/75.5.511.

20. Shah NB, Osmon DR, Fadel H, Patel R, Kohner PC, Steckelberg JM, Mabry T, Berbari EF. 2010. Laboratory and clinical characteristics of *Staphylococcus lugdunensis* prosthetic joint infections. J. Clin. Microbiol. **48**:1600–1603. http://dx.doi.org/10.1128/JCM.01769-09.

21. Murdoch DR, Everts RJ, Chambers ST, Cowan IA. 1996. Vertebral osteomyelitis due to *Staphylococcus lugdunensis*. J. Clin. Microbiol. **34**:993–994.

22. Vigna F, Stracher M, Auerbach A, Suss A, Majid K, Spero C. 2007. *Staphylococcus lugdunensis* osteomyelitis: a case report. Am. J. Orthop. (Belle Mead NJ) **36**:E3–E4.

23. Mei-Dan O, Mann G, Steinbacher G, Ballester SJ, Cugat RB, Alvarez PD. 2008. Septic arthritis with *Staphylococcus lugdunensis* following arthroscopic ACL revision with BPTB allograft. Knee Surg. Sports Traumatol. Arthrosc. **16**:15–18. http://dx.doi.org/10.1007/s00167-007-0379-8.

24. Arias M, Tena D, Apellániz M, Asensio MP, Caballero P, Hernández C, Tejedor F, Bisquert J. 2010. Skin and soft tissue infections caused by *Staphylococcus lugdunensis*: report of 20 cases. Scand. J. Infect. Dis. **42**:879–884. http://dx.doi.org/10.3109/00365548.2010.509332.

25. Liu PY, Huang YF, Tang CW, Chen YY, Hsieh KS, Ger LP, Chen YS, Liu YC. 2010. *Staphylococcus lugdunensis* infective endocarditis: a literature review and analysis of risk factors. J. Microbiol. Immunol. Infect. **43**:478–484. http://dx.doi.org/10.1016/S1684-1182(10)60074-6.

26. Moriarty TF, Campoccia D, Nees SK, Boure LP, Richards RG. 2010. *In vivo* evaluation of the effect of intramedullary nail microtopography on the development of local infection in rabbits. Int. J. Artif. Organs **33**:667–675.

27. Rochford ET, Poulsson AH, Salavarrieta Varela J, Lezuo P, Richards RG, Moriarty TF. 2014. Bacterial adhesion to orthopaedic implant materials and a novel oxygen plasma modified PEEK surface. Colloids Surf. B Biointerfaces **113**:213–222. http://dx.doi.org/10.1016/j.colsurfb.2013.09 .012.

28. Stepanović S, Vuković D, Hola V, Di Bonaventura G, Djukić S, Cirković I, Ruzicka F. 2007. Quantification of biofilm in microtiter plates: overview of testing conditions and practical recommendations for assessment of biofilm production by staphylococci. APMIS **115**:891–899. http://dx.doi.org/10.1111/j.1600-0463.2007.apm_630.x.

29. McDowell A, Barnard E, Nagy I, Gao A, Tomida S, Li H, Eady A, Cove J, Nord CE, Patrick S. 2012. An expanded multilocus sequence typing scheme for *Propionibacterium acnes*: investigation of 'pathogenic', 'commensal' and antibiotic resistant strains. PLoS One **7**:e41480. http://dx.doi .org/10.1371/journal.pone.0041480.

30. McDowell A, Gao A, Barnard E, Fink C, Murray PI, Dowson CG, Nagy I, Lambert PA, Patrick S. 2011. A novel multilocus sequence typing scheme for the opportunistic pathogen *Propionibacterium acnes* and characterization of type I cell surface-associated antigens. Microbiology **157**:1990–2003. http://dx.doi.org/10.1099/mic.0.049676-0.

31. Valanne S, McDowell A, Ramage G, Tunney MM, Einarsson GG, O'Hagan S, Wisdom GB, Fairley D, Bhatia A, Maisonneuve JF, Lodes M, Persing DH, Patrick S. 2005. CAMP factor homologues in *Propionibacterium acnes*: a new protein family differentially expressed by types I and II. Microbiology **151**:1369–1379. http://dx.doi.org/10.1099/mic.0 .27788-0.

32. Lodes MJ, Secrist H, Benson DR, Jen S, Shanebeck KD, Guderian J, Maisonneuve JF, Bhatia A, Persing D, Patrick S, Skeiky YA. 2006. Variable expression of immunoreactive surface proteins of *Propionibacterium acnes*. Microbiology **152**:3667–3681. http://dx.doi.org/10.1099/mic .0.29219-0.

33. McDowell A, Valanne S, Ramage G, Tunney MM, Glenn JV, McLorinan GC, Bhatia A, Maisonneuve JF, Lodes M, Persing DH, Patrick S. 2005. *Propionibacterium acnes* types I and II represent phylogenetically distinct groups. J. Clin. Microbiol. **43**:326–334. http://dx.doi.org/10.1128/JCM.43 .1.326-334.2005.

34. Tunney MM, Patrick S, Gorman SP, Nixon JR, Anderson N, Davis RI, Hanna D, Ramage G. 1998. Improved detection of infection in hip replacements. A currently underestimated problem. J. Bone Joint Surg. Br. **80**:568–572. http://dx.doi.org/10.1302/0301-620X.80B4.8473.

35. Butler-Wu SM, Burns EM, Pottinger PS, Magaret AS, Rakeman JL, Matsen FA, III, Cookson BT. 2011. Optimization of periprosthetic culture for diagnosis of *Propionibacterium acnes* prosthetic joint infection. J. Clin. Microbiol. **49**:2490–2495. http://dx.doi.org/10.1128/JCM.00450-11.

36. Levitt MR, Gabikian P, Pottinger PS, Silbergeld DL. 2011. *Propionibacterium acnes* osteomyelitis occurring 23 years after craniotomy: case report and review of literature. Neurosurgery **69**:E773–E779. http://dx.doi.org /10.1227/NEU.0b013e31821964ba.

37. Piper KE, Jacobson MJ, Cofield RH, Sperling JW, Sanchez-Sotelo J, Osmon DR, McDowell A, Patrick S, Steckelberg JM, Mandrekar JN, Fernandez Sampedro M, Patel R. 2009. Microbiologic diagnosis of prosthetic shoulder infection by use of implant sonication. J. Clin. Microbiol. **47**:1878–1884. http://dx.doi.org/10.1128/JCM.01686-08.

38. Pottinger P, Butler-Wu S, Neradilek MB, Merritt A, Bertelsen A, Jette JL, Warme WJ, Matsen FA, III. 2012. Prognostic factors for bacterial cultures positive for *Propionibacterium acnes* and other organisms in a large series of revision shoulder arthroplasties performed for stiffness, pain, or loosening. J. Bone Joint Surg. Am. **94**:2075–2083. http://dx.doi .org/10.2106/JBJS.K.00861.

39. Patrick S, McDowell A, Glenn JV, Tunney MM. 2008. Improved detection and treatment of prosthetic joint infection. Eur. Cells Mater. **16**(Suppl 2):1.

40. Blomgren G, Lundquist H, Nord CE, Lindgren U. 1981. Late anaerobic haematogenous infection of experimental total joint replacement. A study in the rabbit using *Propionibacterium acnes*. J. Bone Joint Surg. Br. **63B**:614–618.

41. Ferguson KP, Lambe DW, Jr, Keplinger JL, Kalbfleisch JH. 1991. Comparison of the pathogenicity of three species of coagulase-negative *Staphylococcus* in a mouse model with and without a foreign body. Can. J. Microbiol. **37**:722–724. http://dx.doi.org/10.1139/m91-124.

42. Lambe DW, Jr, Ferguson KP, Keplinger JL, Gemmell CG, Kalbfleisch JH. 1990. Pathogenicity of *Staphylococcus lugdunensis*, *Staphylococcus schleiferi*, and three other coagulase-negative staphylococci in a mouse model and possible virulence factors. Can. J. Microbiol. **36**:455–463. http: //dx.doi.org/10.1139/m90-080.

43. Rozalska B, Ljungh A. 1995. Biomaterial-associated staphylococcal peritoneal infections in a neutropaenic mouse model. FEMS Immunol. Med. Microbiol. **11**:307–319.

44. Chassain B, Lemée L, Didi J, Thiberge JM, Brisse S, Pons JL, Pestel-Caron M. 2012. Multilocus sequence typing analysis of *Staphylococcus lugdunensis* implies a clonal population structure. J. Clin. Microbiol. **50**:3003–3009. http://dx.doi.org/10.1128/JCM.00988-12.

45. Andriole VT, Nagel DA, Southwick WO. 1973. A paradigm for human chronic osteomyelitis. J. Bone Joint Surg. Am. **55**:1511–1515.

46. Norden CW. 1970. Experimental osteomyelitis. I. A description of the model. J. Infect. Dis. **122**:410–418. http://dx.doi.org/10.1093/infdis/122.5 .410.

47. Kanellakopoulou K, Galanopoulos I, Soranoglou V, Tsaganos T, Tziortzioti V, Maris I, Papalois A, Giamarellou H, Giamarellos-Bourboulis EJ. 2009. Treatment of experimental osteomyelitis caused by methicillin-resistant *Staphylococcus aureus* with a synthetic carrier of calcium sulphate (Stimulan) releasing moxifloxacin. Int. J. Antimicrob. Agents **33**:354–359. http://dx.doi.org/10.1016/j.ijantimicag.2008.09.008.

48. Petty W, Spanier S, Shuster JJ, Silverthorne C. 1985. The influence of skeletal implants on incidence of infection. Experiments in a canine model. J. Bone Joint Surg. Am. **67**:1236–1244.

49. Smeltzer MS, Thomas JR, Hickmon SG, Skinner RA, Nelson CL, Griffith D, Parr TR, Jr, Evans RP. 1997. Characterization of a rabbit model of staphylococcal osteomyelitis. J. Orthop. Res. **15**:414–421. http: //dx.doi.org/10.1002/jor.1100150314.

50. Heilbronner S, Holden MT, van Tonder A, Geoghegan JA, Foster TJ, Parkhill J, Bentley SD. 2011. Genome sequence of *Staphylococcus lugdunensis* N920143 allows identification of putative colonization and virulence factors. FEMS Microbiol. Lett. **322**:60–67. http://dx.doi.org/10 .1111/j.1574-6968.2011.02339.x.

51. Broekhuizen CA, Sta M, Vandenbroucke-Grauls CM, Zaat SA. 2010. Microscopic detection of viable *Staphylococcus epidermidis* in periimplant tissue in experimental biomaterial-associated infection, identified by bromodeoxyuridine incorporation. Infect. Immun. **78**:954–962. http: //dx.doi.org/10.1128/IAI.00849-09.

52. Palmer M, Costerton W, Sewecke J, Altman D. 2011. Molecular techniques to detect biofilm bacteria in long bone nonunion: a case report. Clin. Orthop. Relat. Res. **469**:3037–3042. http://dx.doi.org/10.1007/s11999-011-1843-9.

53. **Bayston R, Ashraf W, Barker-Davies R, Tucker E, Clement R, Clayton J, Freeman BJ, Nuradeen B.** 2007. Biofilm formation by *Propionibacterium acnes* on biomaterials *in vitro* and *in vivo*: impact on diagnosis and treatment. J. Biomed. Mater. Res. A **81**:705–709. http://dx.doi.org/10.1002/jbm.a.31145.

54. **Holmberg A, Lood R, Mörgelin M, Söderquist B, Holst E, Collin M, Christensson B, Rasmussen M.** 2009. Biofilm formation by *Propionibacterium acnes* is a characteristic of invasive isolates. Clin. Microbiol. Infect. **15**:787–795. http://dx.doi.org/10.1111/j.1469-0691.2009.02747.x.

55. **Ramage G, Tunney MM, Patrick S, Gorman SP, Nixon JR.** 2003. Formation of *Propionibacterium acnes* biofilms on orthopaedic biomaterials and their susceptibility to antimicrobials. Biomaterials **24**:3221–3227. http://dx.doi.org/10.1016/S0142-9612(03)00173-X.

56. **Tunney MM, Dunne N, Einarsson G, McDowell A, Kerr A, Patrick S.** 2007. Biofilm formation by bacteria isolated from retrieved failed prosthetic hip implants in an *in vitro* model of hip arthroplasty antibiotic prophylaxis. J. Orthop. Res. **25**:2–10. http://dx.doi.org/10.1002/jor.20298.

57. **Niazi SA, Clarke D, Do T, Gilbert SC, Mannocci F, Beighton D.** 2010. *Propionibacterium acnes* and *Staphylococcus epidermidis* isolated from refractory endodontic lesions are opportunistic pathogens. J. Clin. Microbiol. **48**:3859–3869. http://dx.doi.org/10.1128/JCM.01326-10.

58. **Carneiro S, Sampaio-Barros PD.** 2013. SAPHO syndrome. Rheum. Dis. Clin. North Am. **39**:401–418. http://dx.doi.org/10.1016/j.rdc.2013.02.009.

59. **Schaeverbeke T, Lequen L, de Barbeyrac B, Labbé L, Bébéar CM, Morrier Y, Bannwarth B, Bébéar C, Dehais J.** 1998. *Propionibacterium acnes* isolated from synovial tissue and fluid in a patient with oligoarthritis associated with acne and pustulosis. Arthritis Rheum. **41**:1889–1893. http://dx.doi.org/10.1002/1529-0131(199810)41:10<1889::AID-ART23>3.0.CO;2-F.

60. **Weisburg WG, Barns SM, Pelletier DA, Lane DJ.** 1991. 16S ribosomal DNA amplification for phylogenetic study. J. Bacteriol. **173**:697–703.

61. **Szabados F, Nowotny Y, Marlinghaus L, Korte M, Neumann S, Kaase M, Gatermann SG.** 2011. Occurrence of genes of putative fibrinogen binding proteins and hemolysins, as well as of their phenotypic correlates in isolates of *S. lugdunensis* of different origins. BMC Res. Notes **4**:113. http://dx.doi.org/10.1186/1756-0500-4-113.

62. **Minhas T, Ludlam HA, Wilks M, Tabaqchali S.** 1995. Detection by PCR and analysis of the distribution of a fibronectin-binding protein gene (*fbn*) among staphylococcal isolates. J. Med. Microbiol. **42**:96–101. http://dx.doi.org/10.1099/00222615-42-2-96.

63. **Noguchi N, Goto K, Ro T, Narui K, Ko M, Nasu Y, Utsumi K, Takazawa K, Moriyasu F, Sasatsu M.** 2010. Using the tannase gene to rapidly and simply identify *Staphylococcus lugdunensis*. Diagn. Microbiol. Infect. Dis. **66**:120–123. http://dx.doi.org/10.1016/j.diagmicrobio.2009.03.028.

64. **Sandoe JAT, Longshaw CM.** 2001. Ventriculoperitoneal shunt infection caused by *Staphylococcus lugdunensis*. Clin. Microbiol. Infect. **7**:385–387. http://dx.doi.org/10.1046/j.1198-743x.2001.00268.x.